of the organochromium cation? The alkyl group of $(H_2O)_5CrR^{2+}$ complexes is known to labilize the trans water to a very substantial extent.[47] Experiments to determine directly the substitution rate were done using its anation reaction with NCS^-:

$$(H_2O)_5CrCH(CH_3)_2^{2+} + NCS^- = (H_2O)_4(SCN)CrCH(CH_3)_2^+ + H_2O \quad (32)$$

The value[48] at 25.0 °C is $k_{32} = 1.25 \pm 0.02\ M^{-1}\ s^{-1}$, far less than required ($k_{3A} = 6.4 \times 10^4\ M^{-1}\ s^{-1}$) to have the trans-accelerated ligand substitution reaction provide a pathway for S_H2 attack by $(CH_3)_2COO\cdot$. (This argument presumes that the same limits found for nucleophilic substitution reactions such as eq 32 govern the rate constants for homolytic displacement, which is not necessarily the case.)

The homolytic displacement may instead occur by simultaneous displacement of the alkyl group by the entering peroxy. That is to say, the mechanism might be a bimolecular displacement process rather than the unimolecular reaction of an intermediate such as $ROOCrR^{2+}$ formed in a prior substitution step.

Products of Autoxidation. If we accept, on the basis of the arguments given above, that the chain-propagation steps produce the (alkylperoxo)chromium(III) ion, then its subsequent reactions account for all the products formed. The yields given in Table VI refer to experiments run under conditions where the chain process predominates. When that is the case, the appreciable yield of 2-propanol is not exclusively that produced by the termination step of mechanism A, since (given the chain length) only some 1-1.5% could be so produced. Likewise, of the 10% of so of chromium(VI) found, only a comparably small amount might be formed via eq 33 from oxidation of the Cr^{2+} (the product shown

$$Cr^{2+} \xrightarrow{O_2} CrO_2^{2+} \xrightarrow{2H_2O} HCrO_4^- + 3H^+ \quad (33)$$

in eq 33 is a minor one in any case) which is a product of the homolysis reaction. The appreciable yields suggest another explanation must be sought.

We suggest that $CrOOCH(CH_3)_2^{2+}$ decomposes by reaction with H^+ to two independent products, acetone (eq 5) and 2-propyl hydroperoxide (eq 34). The analogous cobaloxime complex

$$(H_2O)_5CrOOCH(CH_3)_2^{2+} + H_3O^+ \rightarrow Cr(H_2O)_6^{3+} + (CH_3)_2CHOOH \quad (34)$$

$(CH_3)_2CHOOCo(dmgH)_2L$ is known to react concurrently by two such independent processes.[10] The relative importance of each depends, among other things, on the identity of the ligand L.

The hydroperoxide formed in eq 34 which is not found among the final products—although it has been shown[10] to be stable in aqueous perchloric acid toward decomposition to acetone and water—evidently reacts further. It is likely that 2-propyl hydroperoxide oxidizes Cr(III) species $Cr(H_2O)_6^{3+}$ or Cr_2O^{4+}, accounting for the 2-propanol and $HCrO_4^-$ formed. (The latter substances, although eventually reacting to form acetone and Cr(III), do so very slowly under these conditions.) It would be too tentative, on the basis of the data, for us to speculate as to the detailed steps involved, considering the reactions are undoubtedly quite complex, but the results are not inconsistent with the involvement of reactions such as that given by eq 35.

$$2Cr^{3+} + 3(CH_3)_2CHOOH + 5H_2O = 3(CH_3)_2CHOH + 2HCrO_4^- + 8H^+ \quad (35)$$

Some 10% of the chromium products are dimeric Cr(III) species such as Cr_2O^{4+} or $Cr_2(OH)_2^{4+}$ (Table VI). The reaction of Cr^{2+} and O_2, although known to produce dimers, is probably not responsible under conditions where Cr^{2+} is produced slowly by homolysis in the presence of a large excess of O_2. Under such conditions the CrO_2^{2+} so formed is unlikely to be further converted to $CrOOCr^{4+}$, the latter believed to be the precursor of the stable dimers. Instead, we suggest that reactions of intermediate oxidation states of chromium formed during its reaction with the peroxide as in eq 35 are a more likely source. The suggestion that $HCrO_4^-$ formation largely occurs independently of the reaction with O_2, although closely following it, accounts qualitatively for the wavelength dependence observed.

Acknowledgment. This work was supported by the U.S. Department of Energy, Office of Basic Energy Sciences, Chemical Sciences Division under Contract W-7405-ENG-82. We are pleased to acknowledge helpful discussions with Drs. A. Bakač and M. D. Johnson and the assistance of the Ames Laboratory Analytical Services group for gas chromatographic (J. Richard) and mass spectrometric (G. J. Flesch) analyses.

(47) Bushey, W. R.; Espenson, J. H. *Inorg. Chem.* **1977**, *16*, 2772.
(48) Bakač, A., unpublished results.

Nitrous Acid Decomposition Catalyzed by an Iron(II) Complex: Tris(3,4,7,8-tetramethyl-1,10-phenanthroline)iron(II)[1]

Irving R. Epstein,* Kenneth Kustin,* and Reuben H. Simoyi

Contribution from the Department of Chemistry, Brandeis University, Waltham, Massachusetts 02254. *Received July 20, 1981*

Abstract: In the presence of low concentrations of tris(3,4,7,8-tetramethyl-1,10-phenanthroline)iron(II) ($Fe^{II}TMP$), nitrous acid decomposes to yield nitric oxide and nitrate. The kinetics of this two-stage reaction have been studied by using rapid-mixing techniques. During the first rapid phase, $Fe^{II}TMP$ is oxidized by HNO_2 and by NO_2^- to $Fe^{III}TMP$. The initial ferrous complex is then regenerated in a slower second phase dominated by the reaction of $Fe^{III}TMP$ with NO_2. Rate constants for the reactions of $Fe^{III}TMP$ with nitrous acid and with nitrite were found to be $(7.26 \pm 0.07) \times 10^2\ M^{-1}\ s^{-1}$ and $(2.57 \pm 0.03) \times 10^4\ M^{-1}\ s^{-1}$, respectively, at 25 °C and ionic strength 0.5 M. Computer simulations have been carried out by using a mechanism developed for the hexaaquoiron(II)–nitric acid system, with appropriate modification for the different kinetic properties of the iron species. Quantitative agreement between calculation and experiment is obtained for the first phase, and the model qualitatively predicts the observed regeneration of FeTMP(II) in the second phase.

The surprisingly complex oxidation of aquoiron(II) ion by nitric acid has recently been the subject of a systematic kinetics study.[2] The slow direct reaction between hexaaquoiron(II) and nitrate was found to be of minor importance in that system. Once the

0002-7863/82/1504-0712$01.25/0

Table I. Reduction Potentials[5] for the Oxynitrogen- and Iron-Containing Species[a]

number	reaction	E_1^0, V
E1	$NO_3^- + 3H^+ + 2e^- \rightleftharpoons HNO_2 + H_2O$	0.94
E2	$NO_3^- + 4H^+ + 3e^- \rightleftharpoons NO + 2H_2O$	0.96
E3	$2NO_3^- + 4H^+ + 2e^- \rightleftharpoons N_2O_4 + 2H_2O$	0.80
E4	$N_2O_4 + 2H^+ + 2e^- \rightleftharpoons 2HNO_2$	1.07
E5	$N_2O_4 + 4H^+ + 4e^- \rightleftharpoons 2NO + 2H_2O$	1.03
E6	$HNO_2 + H^+ + e^- \rightleftharpoons NO + H_2O$	1.00
E7	$Fe(H_2O_6)^{3+} + e^- \rightleftharpoons Fe(H_2O)_6^{2+}$	0.771
E8	$Fe^{III}TMP + e^- \rightleftharpoons Fe^{II}TMP$	0.81[b]

[a] Standard states for all species are 1 M aqueous, with the exception of N_2O_4 and NO, for which the standard state is the gas phase. [b] Brandt, W. W.; Smith, G. F. *Anal. Chem.* 1949, *21*, 1313–1319.

reaction starts, *nitrous* acid plays the pivotal role in determining the kinetics of the overall reaction.

Coordination of iron(II) by strong field ligands has a pronounced effect on the electron-donating ability of this reducing agent, making it much more reactive than the aquated ferrous ion.[3] Changes in redox potential also follow changes in coordination and may result in a species thermodynamically incapable of reducing nitric and/or nitrous acid. The autocatalytic iron(II)–nitric(ous) acid reaction has been of considerable interest to us as a possible component in a new chemical oscillator. The fact that the reaction exhibits bistability in a flow reactor[4] enhances this possibility. We therefore wished to probe how changes in the properties of the iron moiety might modify the overall kinetics of the system.

In order to focus on the kinetic effects of complexation, we sought an iron(II) complex with an oxidation potential near that of $Fe(H_2O)_6^{2+}$. Tris(3,4,7,8-tetramethyl-1,10-phenanthroline)-iron(II) ($Fe^{II}TMP$) has a potential within 0.04 V of the hexaaquo species and was thus chosen for this investigation. Initial studies showed that $Fe^{II}TMP$ reacts more rapidly with nitric acid than does hexaaquoiron(II), mainly because of the greater speed of the iron(II)–nitrous acid reaction. Since the reaction of the iron species with HNO_2 appears to be the key to both reactions, a detailed kinetics examination of the nitrous acid oxidation of $Fe^{II}TMP$ was undertaken.

This reaction, though fast, and thus requiring the use of rapid mixing to study part of the time course, is a complex, two-stage process. As in the case of the hexaaquoiron(II)–nitric acid reaction, computer simulation has been used to elucidate the kinetics of the reaction we are reporting. For facilitation of an understanding of this system, the reduction potentials of the different oxynitrogen- and iron-containing species that will eventually be considered are collected in Table I.[5] The major reactions taking place in the hexaaquoiron(II)–nitric acid reaction, which also play a role in this study, are listed in Table II, together with their important kinetics parameters.

Reaction between hexaaquoiron(II) and nitric acid is slow, requiring several minutes to go to completion, depending on concentration, pH, and temperature. The reaction exhibits three phases: a slow induction period, an accelerating autocatalytic phase, and a rapid shutdown. Reaction between hexaaquoiron(II) and nitrous acid, the subject of a definitive kinetics study by Abel and co-workers,[6] is also slow enough to be measured by classical techniques and is monophasic, with a three-term rate law. The reaction between $Fe^{II}TMP$ and nitrous acid is quite different from either of the two previous reactions.

Table II. The Major Reactions and Rate Expressions Employed in Simulations of the $Fe(H_2O)_6^{2+}$–HNO_3 System[a]

$$Fe^{2+} + NO_3^- + 2H^+ \rightleftharpoons Fe^{3+} + NO_2 + H_2O \quad (P1)$$
$$v_1 = (1.5 \times 10^{-4}\ M^{-1}\ s^{-1})[Fe^{2+}][NO_3^-]$$
$$v_{-1} = (2.1 \times 10^{-2}\ M\ s^{-1})[Fe^{3+}][NO_2]/[H^+]^2$$

$$Fe^{2+} + NO_2 + H^+ \rightleftharpoons Fe^{3+} + HNO_2 \quad (P2)$$
$$v_2 = (3.1 \times 10^4\ M^{-1}\ s^{-1})[Fe^{2+}][NO_2]$$
$$v_{-2} = (6.6 \times 10^{-4}\ s^{-1})[Fe^{3+}][HNO_2]/[H^+]$$

$$Fe^{2+} + HNO_2 + H^+ \rightleftharpoons Fe^{3+} + NO + H_2O \quad (P3)$$
$$v_3 = [(7.8 \times 10^{-3}\ M^{-1}\ s^{-1}) + (2.3 \times 10^{-1}\ M^{-2}\ s^{-1})[H^+] + (7.6 \times 10^{-3}\ M^{-1}\ s^{-1})[HNO_2]/[NO]][Fe^{2+}][HNO_2]$$
$$v_{-3} = [(5.6 \times 10^{-4}\ s^{-1})[NO]/[H^+] + (1.6 \times 10^{-2}\ M^{-1}\ s^{-1})[NO] + (5.4 \times 10^{-4}\ s^{-1})[HNO_2]/[H^+]][Fe^{3+}]$$

$$Fe^{2+} + NO \rightleftharpoons FeNO^{2+} \quad (P4)$$
$$v_4 = (6.2 \times 10^5\ M^{-1}\ s^{-1})[Fe^{2+}][NO]$$
$$v_{-4} = (1.4 \times 10^3\ s^{-1})[FeNO^{2+}]$$

$$2NO_2 + H_2O \rightleftharpoons HNO_2 + NO_3^- + H^+ \quad (P5)$$
$$v_5 = (1.7 \times 10^8\ M^{-1}\ s^{-1})[NO_2]^2$$
$$v_{-5} = (2.7 \times 10^{-2}\ M^{-2}\ s^{-1})[HNO_2][NO_3^-][H^+]$$

$$2HNO_2 \rightleftharpoons NO + NO_2 + H_2O \quad (P6)$$
$$v_6 = (5.8\ M^{-1}\ s^{-1})[HNO_2]^2$$
$$v_{-6} = (2.0 \times 10^7\ M^{-1}\ s^{-1})[NO][NO_2]$$

$$NO_3^- + NO + H^+ \rightleftharpoons NO_2 + HNO_2 \quad (P7)$$
$$v_7 = (7.5\ M^{-3}\ s^{-1})[NO_3^-][NO][H^+]$$
$$v_{-7} = (1.4 \times 10^4\ M^{-2}\ s^{-1})[HNO_2][NO_2]$$

[a] Values for all species in aqueous solution with ionic strength extrapolated to zero taken from ref 2 with correction made for more recent values of NO_2 solubility.

Upon mixing $Fe^{II}TMP$ with nitrous acid, the reddish color of the iron complex rapidly disappears, usually in milliseconds, depending on conditions. The solution turns blue, giving evidence of the formation of $Fe^{III}TMP$—the corresponding ferric complex. This reaction is followed by recovery of the original reddish coloration, the iron(III) product having been almost fully reduced to the original iron(II) complex in 1–2 s. These observations correspond to those of the homogeneous catalysis of nitrous acid decomposition by the $Fe^{II}TMP$ complex.

Experimental Section

Materials. The following reagent grade chemicals were used without further purification: iron(II) tris(3,4,7,8-tetramethyl-1,10-phenanthroline) sulfate (G. F. Smith), sodium nitrite, sodium chloride, hydrochloric acid, and nitric acid (Fisher). To avoid precipitation of the complex, we did not employ nitric acid and perchloric acid as the sources of H^+ ions. Sodium chloride was used as the inert electrolyte to maintain the ionic strength at 0.5 M. The nitrous acid was prepared in situ.

Spectrophotometric Analysis. Changes in the absorbance of the complexes were monitored. The ferrous complex is reddish (extinction coefficient = 13 800 $cm^{-1}\ M^{-1}$),[7,8] with the absorption maximum at λ = 500 nm, while the ferric complex is intense blue and absorbs maximally at λ = 360 nm. Spectra were taken on a Beckman Model 25 spectrophotometer of the ferrous complex before the start of the reaction and at the end of the reaction. These two spectra are identical, showing that the ferrous complex is regenerated.

Stopped Flow. The stopped-flow apparatus uses a pneumatic drive to push the reactant-containing syringes with approximately 31.7 psi in excess of atmospheric pressure. The dead time was measured for the iron(III)–thiocyanate reaction and was found to be 0.003 s. Reactions were followed spectrophotometrically by using a tungsten–halogen light source, a Farrand monochromator, and an RCA 1P28 photomultiplier. The path length was 0.91 cm. Solutions in the pushing syringes were thermostated at 25.0 ± 0.1 °C.

The trace from the photomultiplier is captured and digitalized on a Biomation 610B transient recorder. A computer program plots the trace on a semilog scale and calculates the slope and the intercept. A statistical analysis is done, and any runs that give parameters outside the range of $\pm 2\sigma$ are discarded.

Procedure. Reactant solutions used in the stopped-flow experiments were prepared in two vessels: Vessel A contained the ferrous complex

(1) Part 6 in the series, Systematic Design of Chemical Oscillators. Part 5: Dateo, C. E.; Orbán, M.; DeKepper, P.; Epstein, I. R. *J. Am. Chem. Soc.*, in press.
(2) Epstein, I. R.; Kustin, Warshaw, L. J. *J. Am. Chem. Soc.* **1980**, *102*, 3751–3758.
(3) Weston, R. E., Jr.; Schwarz, H. A. "Chemical Kinetics"; Prentice-Hall: Englewood Cliffs, NJ, 1972; p 213.
(4) Orbán, M.; Kustin, K.; Epstein, I. R., to be published.
(5) Latimer, W. M. "Oxidation Potentials", 2nd ed.; Prentice-Hall: Englewood Cliffs, NJ, 1952.
(6) Abel, E.; Schmid, H.; Pollak, F. *Monatsh. Chem.* **1936**, *69*, 125–143.
(7) Ford-Smith, M. H.; Sutin, N. *J. Am. Chem. Soc.* **1961**, *83*, 1830–1834.
(8) McCurdy, W.H.; Smith, G. F. *Analyst (London)* **1952**, *77*, 846–858.

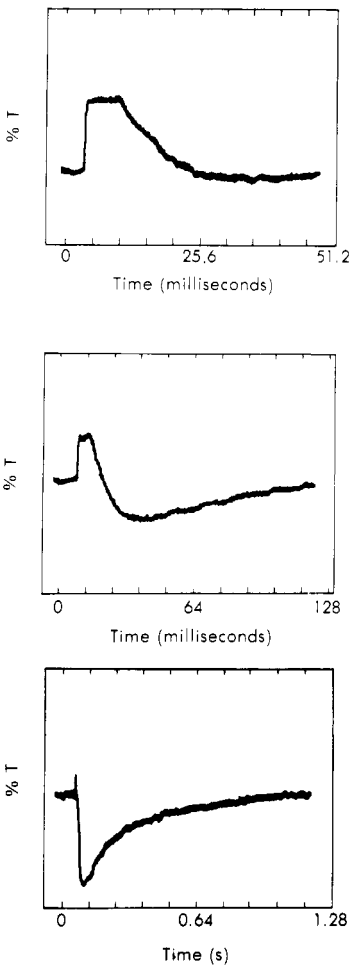

Figure 1. Typical traces of percent transmittance at 500 nm vs. time for the $Fe^{II}TMP$–HNO_2 reaction using three different time spans. Note how the shortest time span shows only the first phase, while the longest enables us to focus on the second (recovery) phase.

and hydrochloric acid, while vessel B had sodium nitrite and sodium chloride. Stock solutions of the complex were prepared by dissolving about 0.26 g of the complex in 250 mL of water. Solutions were then characterized spectrophotometrically. The stock solutions were protected from light by wrapping the flask in aluminum foil.

Reagent solutions were used immediately after preparation so as to minimize the extent of ferrous complex hydrolysis. Doubly distilled water was employed for all the experiments. Standardization of the hydrochloric acid was done at regular intervals with standard sodium hydroxide (Fisher, 0.1 N) and methyl orange as indicator.

Results

All experiments were carried out in the pH range from 1.0 to 4.5 at ionic strength 0.5 M with a large excess of nitrous acid ($\sim 10^{-2}$ M) over the ferrous complex ($\sim 10^{-4}$ M). The pK_a of HNO_2 was taken as 3.35.[9]

When the initial concentration of NO_2^- exceeded that of H^+, no reaction of the ferrous complex was observed. Several series of experiments were done with $[H^+]_0 \geq [NO_2^-]_0$ in an attempt to elucidate the effects of $[H^+]$, $[NO_2^-]$, and $[HNO_2]$ on each of the two phases. Since the first phase (oxidation of $Fe^{II}TMP$) is typically complete in 0.05–0.1 s, while the second phase (regeneration of the ferrous species) generally takes 1–2 s, the two regimes could be monitored separately under favorable conditions by appropriately setting the time span on the Biomation.

If the solutions were allowed to sit for several hours after the return of the red color (completion of phase 2), a slow fading of the reddish color to a very faint blue could be observed, possibly as a result of hydrolysis of the complex.

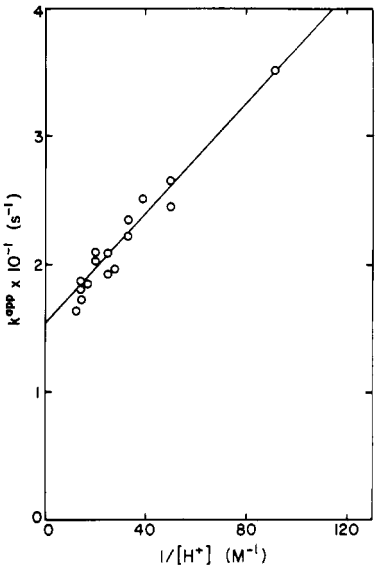

Figure 2. Hydrogen ion dependence of pseudo-first-order rate constant k^{app} for the disappearance of $Fe^{II}TMP$ (phase 1). $[Fe^{II}TMP]_0 = 1.0 \times 10^{-4}$ M, $[NaNO_2]_0 = 2.0 \times 10^{-2}$ M.

First Phase. The first phase was studied at time spans of 0.1 to 0.256 s. Typical results are shown in Figure 1. Efforts were made to determine the dependence of the rate of $Fe^{II}TMP$ consumption on $[H^+]$, $[HNO_2]$, and $[NO_2^-]$.

(a) Hydrogen Ion Dependence. In these experiments, the sodium nitrite and $Fe^{II}TMP$ initial concentrations were kept constant at 2×10^{-2} and 1×10^{-4} M, respectively, while $[H^+]_0$ (HCl) was varied. For each concentration, 5–10 different traces were averaged to give a pseudo-first-order rate constant, k^{app}, for the disappearance of the complex ($[Fe^{II}TMP]_0 \ll [H^+]_0, [NO_2^-]_0$). The experimental values are shown in Figure 2. In contrast to most nitrous acid oxidations,[6,10,11] the rate is observed to decrease with $[H^+]$. The data fit a relation of the form:

$$k^{app} = \frac{a}{[H^+]} + b \qquad (1)$$

Data were analyzed only for $[H^+] < 0.1$ M, because of the instability of nitrous acid at higher acidities. On standing for several minutes, such acidic solutions give rise to bubbles of an odorous gas, probably NO_2. It is unlikely that appreciable decomposition of HNO_2 would have occurred during the brief time span of our rapid-mixing experiments on less acidic solutions.

(b) Nitrous Acid Dependence. A series of experiments was undertaken with equal initial concentrations of $[H^+]$ and $[NO_2^-]$. It was found under these conditions that no clear separation between the first and second phases could be made, as the recovery of the red $Fe^{II}TMP$ color began only a short way into the initial phase. If the conditions were changed so that $[H^+]_0 > [NO_2^-]_0$, the start of the second phase was delayed enough to afford a relatively unambiguous separation between the phases.

A series of experiments was performed in which the difference $[H^+]_0 - [NO_2^-]_0$ was held fixed at 0.02 M, while the two concentrations were varied in order to provide a range of $[HNO_2]$ values. Allowance was made for the ionization of HNO_2. The results, which are of the form $k^{app} = c[HNO_2]$, are summarized in Figure 3.

(c) Nitrite Dependence. Our attempts to determine directly the dependence of k^{app} on $[NO_2^-]_0$ failed because no reaction could be observed with $[NO_2^-]_0 > [H^+]_0$.

(9) Vogel, A. I. "Quantitative Inorganic Analysis", 3rd ed.; Wiley: New York, 1961; p 1168.

(10) Ogino, H.; Tsukahara, K.; Tanaka, N. *Bull. Chem. Soc. Jpn.* **1974**, *47*, 308–311.

(11) Hughes, M. N.; Phillips, E. D.; Stedman, G.; Whincup, P. A. E. *J. Chem. Soc. A* **1969**, 1148–1151.

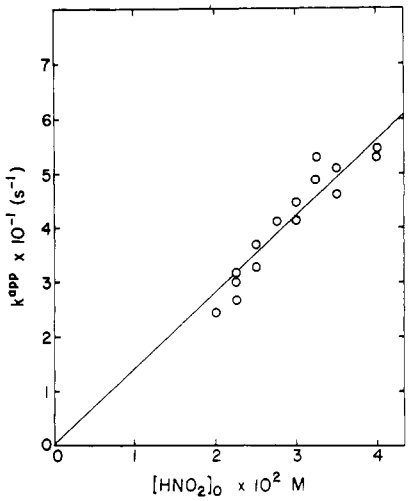

Figure 3. $[HNO_2]$ dependence of k^{app} for phase 1. $[Fe^{II}TMP]_0 = 1.0 \times 10^{-4}$ M, $[HCl]_0 - [NaNO_2]_0 = 0.02$ M.

(d) Rate Constants. The $[H^+]$ dependence of the first phase suggests at least two plausible routes for the oxidation of $Fe^{II}TMP$:

$$Fe^{II}TMP + HNO_2 + H^+ \underset{k'}{\overset{k}{\rightleftharpoons}} Fe^{III}TMP + NO + H_2O \quad (A)$$

$$Fe^{II}TMP + NO_2^- + 2H^+$$

If each pathway in this mechanism proceeds via a rate-determining electron transfer from the complex to the nitrogen species, then, neglecting the back reactions, the pseudo-first-order rate constant for $Fe^{II}TMP$ consumption is given by

$$k^{app} = \left(\frac{k[H^+] + k'K_a}{[H^+] + K_a} \right) C_N^0 \quad (2)$$

where C_N^0 is the total concentration of nitrite-containing species, $[HNO_2] + [NO_2^-]$, and K_a is the acid dissociation constant of nitrous acid.

In our hydrogen ion dependence experiments (Figure 2), $[H^+]_0$ always exceeded $K_a = 4.5 \times 10^{-4}$ by at least a factor of 30. Under these conditions eq 2 may be simplified to

$$k^{app} = \left(k + \frac{k'K_a}{[H^+]} \right) C_N^0 \quad (3)$$

which is of the same form as eq 1. We thus identify a in eq 1 with $k'K_aC_N^0$ and b with kC_N^0. A linear least-squares analysis of the data yielded the following values for the rate constants:

$$k = 7.26 \times 10^2 \text{ M}^{-1} \text{ s}^{-1} \quad (4)$$

$$k' = 2.57 \times 10^4 \text{ M}^{-1} \text{ s}^{-1} \quad (5)$$

with relative errors for k and k' of $\pm 1\%$. Rate constants obtained from the $[HNO_2]$ dependence experiments agreed with those given above to within 0.5%.

Second Phase. The second phase, since it starts well into this rather complex reaction, is considerably more difficult to study experimentally. The starting point in time of this phase as well as the concentrations (and even the identities) of the reactive species defy exact determination. Nevertheless, efforts were made to obtain at least qualitatively reliable data of the sort measured for the first phase.

Although working at excess $[H^+]$ facilitates study of the first phase by delaying the onset of phase 2, it makes evaluation of the latter phase more difficult because fewer data points are available in the time span of the experiment. When $[H^+]$ was significantly greater than $[NO_2^-]$, as much as 30% of the time span was occupied by an induction period between the phases during which the absorbance remained nearly stationary. The most reliable

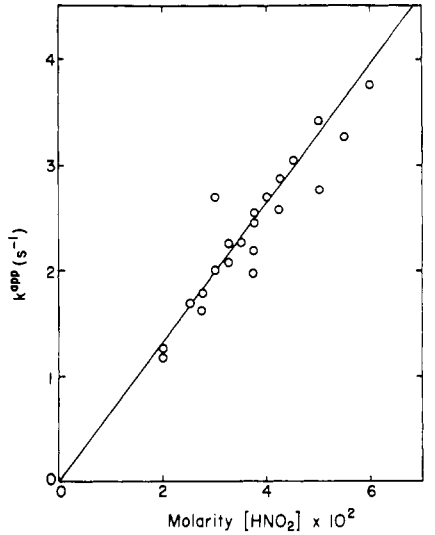

Figure 4. $[HNO_2]$ dependence of k^{app} for phase 2. $[Fe^{II}TMP]_0 = 1.0 \times 10^{-4}$ M, $[HCl]_0 = [NaNO_2]_0$.

results on phase 2 were thus obtained in a series of experiments with $[H^+]_0 = [NO_2^-]_0$.

The results of these experiments are shown in Figure 4. As in the case of the first phase, the pseudo-first-order rate constant varies directly with $[HNO_2]_0$. Efforts to obtain an $[H^+]$ dependence were unsuccessful owing to the large scatter in the data resulting from the difficulties mentioned above when $[H^+]_0 > [NO_2^-]_0$.

Experimentally then, it is difficult to characterize the second phase other than by the recovery of $Fe^{II}TMP$ with time. We therefore undertook to analyze both phases simultaneously by computer simulation of the entire time course of the reaction.

Computer Simulations. To simulate the $Fe^{II}TMP$–nitrous acid system, we employed the set of reactions listed in Table II with several modifications and adjustments. The only independent nitrogen-containing species in this model are NO_3^-, HNO_2, NO, and NO_2. Such species as NO_2^-, N_2O_4, N_2O_3, NO^+, etc. are assumed to be in rapid equilibrium with H^+ and the four independent species. The ionic strength in this study was 0.5 M rather than the 2.1 M used in ref 2. Corrections were made in the appropriate reaction rates by using the Debye–Hückel limiting law expression. A recent study[12] of the behavior of nitrogen dioxide in water at low partial pressure yielded a value of $(7.0 \pm 0.5) \times 10^{-3}$ M atm^{-1} for the Henry's law coefficeint of NO_2, and this value was employed in place of the value 1.9×10^{-2} M atm^{-1} estimated in ref 2. The difference in redox potential between hexaaquoiron(II) and $Fe^{II}TMP$ gives rise to a change in the equilibrium constants of reactions P1–P4.

Reaction rates for steps P5–P7, which do not involve the iron-containing species, were chosen identical with those in the hexaaquoiron(II) study[2] with appropriate corrections for the ionic strength and NO_2 solubility as noted above. The treatment of the reactions involving $Fe^{II}TMP$ is outlined below.

(a) Reaction P1. No quantitative experimental data are available, though the direct reaction of nitrate with $Fe^{II}TMP$ appears to be fairly slow.[13] As in the hexaaquo system, the results of the simulation of Fe(II) consumption are quite insensitive to the value chosen for k_1. However, the choice of k_{-1} had a marked effect on the simulation of the second phase. We therefore selected the value of k_{-1} which gave best agreement for the second phase and used the equilibrium constant for the reaction to determine k_1.

(b) Reaction P2. Again, no direct experimental determination of the rate has been made. We varied k_2 and k_{-2} over a wide range,

(12) Lee, Y.-N.; Schwartz, S. B. *J. Phys. Chem.* **1981**, *85*, 840–848.
(13) Simoyi, R. Ph.D. Thesis, Brandeis University, 1981. Other ferrous complexes such as ferrous 2,2′-bipyridine sulfate and ferrous 4,4′-dimethyl-2,2′-bipyridine sulfate were also found to react sluggishly with nitric acid.

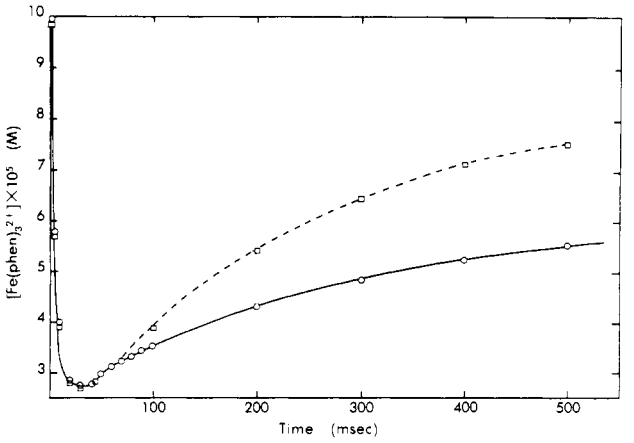

Figure 5. Simulated (○) and experimental (□) time course of the reaction. Initial concentrations: $[Fe^{II}TMP]_0 = 1.0 \times 10^{-4}$ M, $[HNO_2]_0 = 3.0 \times 10^{-2}$ M, $[H^+]_0 = 2.5 \times 10^{-3}$ M.

but the $Fe^{II}TMP-NO_2$ reaction never made any significant contribution to the rate of either phase. We therefore chose k_2 as the value obtained for the hexaaquo system and modified k_{-2} to allow for the change in the equilibrium constant.

(c) Reaction P3. The $Fe^{II}TMP-HNO_2$ reaction constitutes the first phase of the reaction under consideration, and its rate was determined from our data on that phase. Combining eq 3–5 and our value of K_a, we have

$$v_3 = \left(7.26 \times 10^2 + \frac{1.15 \times 10^1}{[H^+]}\right)[Fe^{II}TMP][HNO_2] \quad (6)$$

An expression for v_{-3} may be obtained from eq 6 and the potentials of Table I by requiring each pathway in mechanism A to have the overall equilibrium constant for the reaction (detailed balance).

(d) Reaction P4. While complex formation between Fe(II) and NO is rapid and plays a key role in the hexaaquo system, the extensive coordination around the iron center in $Fe^{II}TMP$ totally suppresses attack by nitric oxide. This reaction plays no role in our system: $v_4 = v_{-4} = 0$.

(e) Results of Simulations. After deletion of (P4), the remaining set of six rate equations was integrated numerically using Hindmarsh's implementation[14] of the Gear method for stiff differential equations.[15] A typical simulation is shown together with the experimental data in Figure 5. We find nearly perfect agreement for the first phase, but the $Fe^{II}TMP$ recovery in the second phase is only partially predicted by the simulation.

The rate constants for reactions P5, P6, P7 were taken from the hexaaquo study; reaction P4 has been eliminated; the parameters for reaction P3 have been established experimentally; and the equilibrium constants for reactions P1 and P2 are known. The model therefore contains only two remaining free parameters, k_1 and k_2. The simulations show, as noted above, no sensitivity to the latter rate constant, because for any reasonable values of k_2 and k_{-2}, we always have $v_2, v_{-2} \ll v_1, v_{-1}, v_3, v_{-3}$. By fitting the experimental time dependence of phase 2, which is quite sensitive to k_{-1}, we obtained an optimal value for k_1 of about 10^3 M^{-1} s^{-1}.

Examination of the rates of the individual reactions as functions of time reveals that the behavior of the system is principally determined by reactions P1, P3, and P6. At all stages of the reaction, we have

$$v_{-1} \gg v_1 \quad (7)$$

$$v_{-1} \approx v_6 \gg v_{-6} \quad (8)$$

$$v_3 > v_{-3} \quad (9)$$

(14) Hindmarsh, A. C. "GEAR: Ordinary Differential Equation System Solver", Technical Report No. U010-3001, Rev. 2; Lawrence Livermore Laboratory: Livermore, CA, 1972.

(15) Gear, C. W. "Numerical Initial Value Problems in Ordinary Differential Equations"; Prentice-Hall: Englewood Cliffs, NJ, 1971; Chapter 11.

Table III. Results of a Numerical Simulation of the $Fe^{II}TMP-HNO_2$ Reaction[a]

	time, ms					
	0	6.6	26.4[c]	100	500	1000
$[Fe^{II}TMP] \times 10^4$ M	1.00	0.50	0.28	0.35	0.55	0.63
$v_{-1} \times 10^3$ M s^{-1}	0.00	3.57	3.52	3.35	2.65	2.07
$v_{-3} \times 10^3$ M s^{-1}	0.00	0.21	0.79	1.71	2.51	2.26
$v_3 \times 10^3$ M s^{-1}	15.9	7.98	4.32	4.95	5.05	4.16
$v_6 \times 10^3$ M s^{-1}	3.60	3.57	3.52	3.34	2.58	1.95
$\Delta[HNO_2] \times 10^3$ M[b]	0.00	−0.12	−0.35	−1.10	−4.60	−7.91
$\Delta[NO_3^-] \times 10^3$ M[b]	0.00	0.02	0.09	0.35	1.52	2.62
$\Delta[NO] \times 10^3$ M[b]	0.00	0.10	0.26	0.76	3.08	5.29
$\Delta[H^+] \times 10^3$ M[b]	0.00	−0.02	0.02	0.28	1.47	2.59

[a] Initial concentrations: $[Fe^{II}TMP]_0 = 1.00 \times 10^{-4}$ M, $[NO_3^-]_0 = [NO_2]_0 = [NO]_0 = 1.00 \times 10^{-7}$ M, $[HNO_2]_0 = 3.00 \times 10^{-2}$ M, $[H^+]_0 = 2.50 \times 10^{-3}$ M. [b] $\Delta[X] = [X] - [X]_0$. [c] End of first phase.

Some typical reaction rates are given in Table III.

During the first phase of the reaction, (P3) is dominant, and $Fe^{II}TMP$ is consumed. Nitrous acid is consumed both by reaction with the ferrous complex in (P3) and by disproportionation in (P6). Essentially all the NO_2 produced by (P6) reacts immediately with any $Fe^{III}TMP$ present in the reverse of (P1) (eq 7–8). Since $[HNO_2]_0 \gg [Fe^{II}TMP]_0$, the ferrous complex concentration decreases significantly during the early stages of the reaction, while $[HNO_2]$ changes only slightly. As a result, after about 30 ms, v_3 has decreased to the point where it no longer exceeds $v_{-1} + v_{-3}$. $Fe^{III}TMP$ is now being reduced as fast as $Fe^{II}TMP$ is oxidized. The first phase is at an end; the second phase is about to begin.

By adding the predominant reactions, −(P1) + (P3) + (P6), we obtain the overall stoichiometry:

$$3HNO_2 = NO_3^- + 2NO + H_2O + H^+ \quad (10)$$

Reaction 10 is simply the decomposition of nitrous acid which was studied by Abel and Schmid[16] in the absence of ferrous species. Under those conditions the reaction proceeds at a considerably slower rate than observed here; $Fe^{II}TMP$ catalyzes the nitrous acid decomposition. Examination of the ratios of changes in species concentrations in the last four rows of Table III shows that after the initial phase, which is characterized primarily by (P3), the stoichiometry is indeed that of reaction 10.

Discussion

Three reaction pathways were found for the hexaaquoiron(II)–nitrous acid reaction,[6] involving electron transfer via direct attack by HNO_2 on the iron center, attack by the intermediate NO^+, and attack by NO_2. In all three cases, the reaction is relatively slow, and inner-sphere mechanisms have been postulated.

The hexaaquochromium(II)–nitrous acid reaction[10] strongly resembles the $Fe^{II}TMP-HNO_2$ reaction both in the order of magnitude of its rate and in the reactive species involved. Two routes of electron transfer exist, one via HNO_2, the other via the conjugate base NO_2^-.

The reaction between $Fe^{II}TMP$ and nitrous acid proceeds much more rapidly than the corresponding hexaaquoiron(II) reaction because the extensive π-conjugated bonding around the iron center provided by the bidentate ligands facilitates the electron-transfer process. Both pathways for the electron transfer presumably involve highly unstable intermediates such as HNO_2^- and its conjugate base NO_2^{2-}, which are rapidly protonated to give nitric oxide and water:

$$Fe^{II}TMP + HNO_2 = Fe^{III}TMP + HNO_2^- \quad \text{(rate-determining step)} \quad (11)$$

$$HNO_2^- + H^+ = H_2O + NO \text{ (fast)} \quad (12)$$

and

(16) Abel, E.; Schmid, H. *Z. Phys. Chem. (Leipzig)* **1928**, *134*, 279–300.

$$Fe^{II}TMP + NO_2^- = Fe^{III}TMP + NO_2^{2-} \quad \text{(rate-determining step)} \quad (13)$$

$$NO_2^{2-} + 2H^+ = H_2O + NO \text{ (fast)} \quad (14)$$

Nitrite attack is faster than nitrous acid attack because of electrostatic and stereochemical considerations. The dipositive charge on the complex favors interaction with anionic species. Nitrite has no hindered side, but HNO_2 cannot accomplish electron transfer through the side that possesses the proton. The inertness of the $Fe^{II}TMP$ coordination shell and the rapidity of the reaction imply that the electron transfer proceeds by an outer-sphere mechanism. Rates of reaction with nitrous acid are in the order $Cr(H_2O)_6^{2+} > Fe^{II}TMP > Fe(H_2O)_6^{2+}$. The hexaaquochromium(II) ion does not have the conjugated π system around the metal center to facilitate electron transfer as in $Fe^{II}TMP$. This lack is apparently compensated, however, by the substantially greater thermodynamic driving force in the chromium–nitrous acid system.

The hexaaquoiron(II)–nitric(ous) acid systems were found to be autocatalytic in the product NO. No evidence of autocatalysis has been found in the present system either in our experimental data or in the simulations. The autocatalytic sequence in the mechanism proposed for the hexaaquoiron system[2] consists of reactions P2, P3, and P7. Apparently, with $Fe^{II}TMP$ the NO_2 produced by (P7) reacts preferentially with the ferric species (which is formed much more rapidly than in the hexaaquo system) via (P1) rather than with $Fe^{II}TMP$ in (P2) as required for the development of autocatalysis.

In spite of limitations on interpretation of the experimental data and on the quantitative agreement between calculation and experiment for phase 2 of the reaction, the present study has provided considerable information about the $Fe^{II}TMP$–nitrous acid system. Rate constants for the reactions of the complex with nitrite and nitrous acid have been determined. A qualitative picture of the origin of the regeneration of the catalyst has been developed. Remarkable agreement has been obtained between the experimental results and those derived from a model for the hexaaquoiron(II)–nitric acid system with the introduction of only a single new adjustable parameter. This investigation also represents one of the first efforts at combining experimental kinetics techniques with numerical simulation to elucidate the nature of homogeneous catalysis.

Acknowledgment. We thank Dr. Irwin Taub for informative discussions. This work was supported by National Science Foundation Grant CHE 7905911 and by NIH Research Grant GM 08893-18.

Registry No. $Fe^{II}TMP$, 17378-70-0; HNO_2, 7782-77-6; NO_2^-, 14797-65-0.

Magnetic Exchange in Imidazolate-Bridged Copper(II) Complexes

Gary Kolks,[1a] Stephen J. Lippard,*[1a] Joseph V. Waszczak,[1b] and Henry R. Lilienthal[1c]

Contribution from the Department of Chemistry, Columbia University, New York, New York 10027, Bell Laboratories, Murray Hill, New Jersey 07974, and the Physical Sciences Department, T. J. Watson Research Center, Yorktown Heights, New York 10598. *Received July 6, 1981*

Abstract: Variable-temperature (4.2–300 K) magnetic susceptibility studies of a variety of imidazolate and substituted imidazolate-bridged dicopper(II) complexes reveal that the imidazolate (im) group can mediate moderate antiferromagnetic interactions. The observed coupling constants (J) for a series of tridentate amine copper(II) complexes in which the bridging ligands are imidazolate, 2-methylimidazolate, benzimidazolate, and 2-methylbenzimidazolate, −26.90 (2), −38.1 (3), −16.99 (1), and −29.82 (4) cm^{-1}, respectively, parallel the first pK_a values of the respective free imidazoles. This behavior is best accounted for by a σ-exchange pathway. Two coupling constants, −87.64 (4) and −35.0 (4) cm^{-1}, are required to fit the data for $[Cu_2(bpim)(im)]_2^{4+}$, a cation having two geometrically distinct imidazolate-bridged dicopper(II) units. Assignment of the coupling constants to their respective bridging imidazolate rings in this tetranuclear cation is achieved by comparison to the J values obtained for Cu_2bpim^{3+} and $[Cu(pip)]_2(im)^{3+}$ (bpim is 4,5-bis[((2-(2-pyridyl)ethyl)imino)methyl]imidazolate and pip is 2-[((2-(2-pyridyl)ethyl)imino)methyl]pyridine). The large negative J value observed for Cu_2bpim^{3+} is rationalized on the basis of the near collinearity of the Cu–N(imidazolate) bonds which increases the through-bond interaction of the nitrogen lone pair orbitals with each other and leads to increased antiferromagnetic coupling. These studies verify the existence of an imidazolate-bridged dicopper(II) center in a form of bovine erythrocyte superoxide dismutase in which Cu(II) replaces Zn(II) and provide a foundation for the identification of imidazolate (histidine) bridged centers in other metallobiomolecules.

Two or more paramagnetic metal atoms bridged by a common diamagnetic ligand may interact via electronic exchange coupling (superexchange) to exhibit overall ferromagnetic or antiferromagnetic behavior.[2-4] Although this behavior can result from metal–metal bonding, the large distance between metal centers (often 3 Å or greater) usually precludes direct overlap of the metal orbitals. In such cases the bridging ligand mediates the exchange interaction providing a pathway through which the metal orbitals can interact.

The exchange-split cluster energy levels are given[2] by the application of the Heisenberg–Dirac–Van Vleck spin-coupling Hamiltonian (eq 1), where J_{ab} is the exchange coupling constant

$$\hat{\mathcal{H}}_{ex} = -2\sum_{a,b} J_{ab}\hat{S}_a\cdot\hat{S}_b \quad (1)$$

for the interaction between metal atoms at sites a and b with total

(1) (a) Columbia University. (b) Bell Laboratories, Murray Hill. (c) IBM Yorktown Heights.
(2) Ginsberg, A. P. *Inorg. Chim. Acta Rev.* **1971**, *5*, 45.
(3) Martin, R. L. In "New Pathways in Inorganic Chemistry", Ebsworth, E. A. V., Maddock, A. G., Sharpe, A. G., eds.; Cambridge University Press: New York, 1968; Chapter 9.
(4) Hodgson, D. J. *Prog. Inorg. Chem.* **1975**, *19*, 173.

0002-7863/82/1504-0717$01.25/0